

Epidemic centrality - is there an underestimated epidemic impact of network peripheral nodes?

Mile Šikić^{1,5,*}, Alen Lančić², Nino Antulov-Fantulin³, Hrvoje Štefančić⁴

1 Bioinformatics Institute, A*STAR, Singapore

2 Faculty of Science, Department of Mathematics, University of Zagreb, Zagreb, Croatia

3 Division of Electronics, Rudjer Bošković Institute, Zagreb, Croatia

4 Theoretical Physics Division, Rudjer Bošković Institute, Zagreb, Croatia

5 Faculty of Electrical Engineering and Computing, University of Zagreb, Zagreb, Croatia

* E-mail: Corresponding mile.sikic@fer.hr

Abstract

In the study of disease spreading on empirical complex networks in SIR model, initially infected nodes can be ranked according to some measure of their epidemic impact. The highest ranked nodes, also referred to as “superspreaders”, are associated to dominant epidemic risks and therefore deserve special attention. In simulations on studied empirical complex networks, it is shown that the ranking depends on the dynamical regime of the disease spreading. A possible mechanism leading to this dependence is illustrated in an analytically tractable example. In systems where the allocation of resources to counter disease spreading to individual nodes is based on their ranking, the dynamical regime of disease spreading is frequently not known before the outbreak of the disease. Therefore, we introduce a quantity called *epidemic centrality* as an average over all relevant regimes of disease spreading as a basis of the ranking. A recently introduced concept of phase diagram of epidemic spreading is used as a framework in which several types of averaging are studied. The epidemic centrality is compared to structural properties of nodes such as node degree, k-cores and betweenness. There is a growing trend of epidemic centrality with degree and k-cores values, but the variation of epidemic centrality is much smaller than the variation of degree or k-cores value. It is found that the epidemic centrality of the structurally peripheral nodes is of the same order of magnitude as the epidemic centrality of the structurally central nodes. The implications of these findings for the distributions of resources to counter disease spreading are discussed.

Author Summary

Studies of disease spreading on complex networks have provided a deep insight into the conditions of onset, dynamics and prevention of epidemics in human populations and malicious software propagation in computer networks. Identifying nodes which, when initially infected, on average infect the largest part of the network and ranking them according to their epidemic impact (the portion of the network eventually infected) is a priority for public health policies. In the study of epidemic spreading on empirical complex networks in the Susceptible-Infected-Recovered model, we find that the required ranking depends on the disease spreading regime, i.e. on how fast the disease is transmitted between nodes and how fast the infected node recovers. A measure called *epidemic centrality*, averaging the epidemic impact over all possible disease spreading regimes, is introduced as a basis of epidemic ranking. We find the epidemic centrality of nodes which are structurally central, to be of the same order of magnitude as the epidemic centrality of structurally peripheral nodes. These findings point to the need to study if the impact of an epidemic starting at structurally peripheral nodes might be considerably underestimated. Network periphery should gain a more prominent role in the study of the allocation of resources in future epidemic preparedness plans.

Introduction

The spreading of contagious diseases represents one of the most dangerous and disruptive phenomena in human communities and animal populations [1, 2]. The propagation of malicious software in computer and communication networks is a technological counterpart of spreading of contagious diseases [3]. The pathways of spreading of detrimental disturbances in these systems are well described by complex networks [4–6]. The dynamics of spreading of diseases on complex networks and mathematical models of such spreading in general [7] make a subject of considerable interest and activity of research community and of big practical importance.

Other forms of spreading are also present in systems described as complex networks. The dissemination of information, formation of public opinion or spreading of fashion proceed in a very similar way as the spreading of diseases, see e.g. section 6.1 in [8]. The studies of these specific forms of social dynamics have attracted a lot of interest of academic community and recently the potential of their commercial application is increasingly coming into focus.

The research on empirical complex networks has revealed their very heterogeneous structure [4–6]. In particular, in scale-free networks the nodes with degrees differing many orders of magnitude may coexist. Therefore, it is not surprising that different nodes have different importance in spreading of disease or information over the network. Finding the nodes that contribute the most to the spreading or the network structures that are the most robust to disease propagation [9] is essential in planning disease control and prevention or devising efficient network marketing strategies. In general, it is important to rank nodes according to their *epidemic impact*. In this paper we refer to such ranking as *epidemic ranking*. The nodes with the highest epidemic impact, frequently referred to as “key players” or “superspreaders”, are usually identified using the structural properties of the underlying complex network. They have been identified with nodes of high degree (hubs) [10–12], high values of k-cores [13] or betweenness centrality [14, 15]. Based on these network structural properties it is possible to construct some ranking of nodes regarding their spreading capabilities. It should be stressed that our definition of superspreading nodes differs somewhat from the concept of superspreaders used in the literature. In epidemiological literature [16–18], the superspreaders are defined as infected nodes which produce a large number of secondary cases (for a precise quantitative definition of a superspreading event see [17]). In this paper we are interested in the type of superspreading at the level of the entire network, i.e. we are interested in initially infected nodes which lead to a large number of infected nodes in the entire network. In this paper we define a “superspreader” as a node which when initially infected, leads to a very large number of infected nodes at the level of the entire network. To emphasize this difference we put quotation marks around the word superspreader. We find this generalization from the secondary cases to the entire network natural and convenient for the present paper.

The spreading dynamics does not depend solely on structural properties. The intensity of spreading of disease is also controlled by properties such as its transmission rate and average infectious period of the infected node. In this paper we adopt the stochastic Susceptible-Infected-Recovered (SIR) epidemiological model [19]. The discrete time stochastic dynamics in this model is controlled by two parameters: p , the probability per time step that the infected node infects a neighboring susceptible node, and q , the probability per time step that the infected node recovers. An important question is how the dynamics of spreading affects the status of “superspreaders” and the epidemic ranking in total. In particular, if the node A has a higher epidemic ranking than the node B in one dynamical regime of spreading (e.g. for SIR model parameters (p_1, q_1)), does the ordering of their rankings (i.e. epidemic impacts) remain the same in some other dynamical regime of spreading (for some other SIR model parameters (p_2, q_2))?

The principal aim of this paper is to study the dependence of the epidemic ranking on the dynamical regime of the disease spreading and compare it to the ranking derived from structure. An important tool in achieving this aim is *the phase diagram of epidemic spreading*, a diagrammatic representation of epidemic impact for all possible epidemic parameter values and for a given network and a given initially infected node [20]. Using the concept of phase diagram of epidemic spreading, a measure of *epidemic*

centrality that takes the spreading dynamics into account is proposed. Finally, the implications to security policies and an optimal allocation of resources are discussed.

In our considerations in this paper we shall assume that the network is static, i.e. that its structure does not change during the course of disease spreading. For a complex network of social contacts this assumption is certainly just a starting approximation since during the outbreak social contacts may in general vary and get restricted [21, 22]. For information and communication networks or spreading of ideas the assumption of static underlying complex network is a much better approximation.

The paper is organized in the following way. The first section is the Introduction. The second section of Materials and Methods comprises three subsections: the first subsection focuses on the dependence of the “superspreader” ranking of a node on the dynamical regime of the disease spreading. The second subsection summarizes the concept of phase diagram of epidemic spreading. In the third subsection the measure of epidemic centrality is introduced. The final section of Results and Discussion is devoted to the analysis of results of simulations on empirical complex networks and their discussion and the paper closes with the summary and conclusions.

Materials and Methods

A majority of results presented in this paper have been obtained by simulations on empirical complex networks. In particular, the following networks have been used: complex network of 2003 condensed matter collaborations (with 27 519 nodes) hereafter referred to as *cond-mat 2003* network [23], an undirected, unweighted network representing the topology of the US Western States Power Grid (having 4941 nodes) hereafter referred to as *power grid* network [24], network of coauthorships between scientists posting preprints on the Astrophysics E-Print Archive between Jan 1, 1995 and December 31, 1999, (consisting of 16 706 nodes) hereafter referred to as *astro-ph* network [23], and a symmetrized snapshot of the structure of the Internet at the level of autonomous systems, reconstructed from BGP tables posted by the University of Oregon Route Views Project (containing 22 963 nodes) hereafter referred to as *internet* network [25]. To complement our research on empirical complex networks, we also perform studies on synthetic Erdos-Renyi (ER) networks. The ER type of networks is chosen to test the concepts introduced in this paper also on networks significantly different from networks with broad degree distributions.

Dependence of the “superspreader” status on the disease spreading dynamical regime

Our principal hypothesis is that the node which is highly ranked as a “superspreader” for some disease spreading parameters (i.e. in some disease spreading regime) may not be highly ranked for some other epidemic parameters (i.e. in some other epidemic regime). More generally, the epidemic ranking of a node i according to its epidemic impact, measured by e.g. the average number of infected nodes for an initially infected node i , is dependent on the dynamics of disease spreading, i.e. parameters describing the spreading of the disease. In this section this hypothesis is tested and supported in two ways. First we present results of simulations on empirical complex networks and then an analytical calculation for a specific artificial network is displayed.

The testing of the hypothesis formulated in the preceding paragraph on empirical complex networks is carried out in the following way. Two pairs of SIR model parameters (p_1, q_1) and (p_2, q_2) are selected. For each node of the empirical complex network and for each pair of the parameter values, the average number of infected nodes (i.e. the final size of the epidemic) for the disease starting at that very node is calculated. In particular for a node i the quantities X_{p_1, q_1}^i and X_{p_2, q_2}^i , the average numbers of infected nodes normalized to the total number of nodes in the network for parameters (p_1, q_1) and (p_2, q_2) , respectively, are obtained. A plot with X_{p_1, q_1}^i and X_{p_2, q_2}^i on the axes is constructed. For each initially infected

node a point is entered into the plot. An example of such a plot obtained for the cond-mat network is presented in Fig. 1.

The scattering of the points in the plot presented in Fig. 1 vividly demonstrates the dependence of the epidemic ranking on the disease spreading regime. In this plot two points A and B have been singled out to show how the ranking of two nodes is altered if the dynamical regime of disease spreading is changed. If there was no dependence of the epidemic ranking on parameters of the disease spreading model, the points in Fig. 1 would be ordered in a monotonously growing curve. Analogous plots demonstrating the dependence of the ranking on the dynamical regime have also been obtained for other studied empirical complex networks and other combinations of (p, q) pairs.

The results of simulations on empirical complex networks presented above clearly illustrate the dependence of the node's ranking according to its epidemic impact on the dynamical regime of spreading. There are many conceivable mechanisms how this dependence might be realized in practice. In the remainder of this section we focus on an analytically tractable example of the disease spreading where we demonstrate one possible mechanism of dependence on the dynamical regime of spreading.

We consider an artificial undirected network dominated by three nodes with high degrees. Let us denote these nodes by 1, 2 and 3 and let their degrees be k_1 , k_2 and k_3 , respectively. One of these nodes, the node 2, has a central position in the network. It is connected to nodes 1 and 3 with chains of length n_1 and n_3 respectively. The nodes connected to one of the nodes 1, 2 and 3 are said to belong to their respective stars. We are interested in the situation where the central node 2 has smaller degree than the nodes 1 and 3, i.e. $k_2 < k_1$ and $k_2 < k_3$. The lengths of the chains are comparable, i.e. $n_1 \simeq n_2$. An example of such a network with $k_1 = 18$, $k_2 = 12$, $k_3 = 20$, $n_1 = 7$ and $n_3 = 4$ is presented in Fig. 2.

The mechanism of disease spreading in this network is relatively simple. Since the network has a tree topology, for an arbitrary initially infected node there is a unique path in the network via which any other node can be infected. For a node to get infected, its neighbor on the path connecting the studied node with the initially infected node must be infected too. A formalism for the full analytical description of the disease spreading in tree-like networks has been recently developed in [20]. In general, we consider a bipartite graph with two classes of nodes. The class I contains s nodes which are all in the infected (I) state. The class II consists of n nodes which are in the susceptible (S) state. Every node from the class I is connected to all nodes from the class II. The probability that the random variable $X_n^{(s)}$, numbering eventually infected nodes in class II, acquires the value k is [20]

$$\begin{aligned} p_{n,k}^{(s)} &\equiv P(X_n^{(s)} = k) = \\ &= q^s \binom{n}{k} \sum_{l=0}^k \binom{k}{l} (-1)^l \left(\frac{(1-p)^{n-k+l}}{1 - (1-q)(1-p)^{n-k+l}} \right)^s. \end{aligned} \quad (1)$$

Using the expression (1), we consider the expected number of infected nodes for two different initially infected nodes. For the scenario in which the spreading of the disease starts from the node 1 the random variable of the number of infected nodes is denoted by Y_1 . For the second scenario in which the spreading begins from the node 2, the respective random variable is denoted by Y_2 . For the calculation of expected values of Y_1 and Y_2 we need a particular instance of (1), namely $P(X_1^{(1)} = 1)$. For a selected initially infected node, in the studied network every node can be infected only from one of its neighbors. Furthermore the process of disease transfer from the infected to the susceptible node is an independent process for all pairs of neighboring nodes consisting of one infected and one susceptible node. The existence of the chain between the nodes 1 and 2 and the chain between the nodes 2 and 3 is the most artificial element of the studied network. It is needed to produce a large illustrative variation of the expectation of $Y_1 - Y_2$. For shorter chains this variation would be smaller, but still present.

The expected value of the number of infected nodes in the first scenario of interest is given with the

following expression:

$$\begin{aligned}
E(Y_1) &= 1 + k_1 P(X_1^{(1)} = 1) + \sum_{i=2}^{n_1+1} (P(X_1^{(1)} = 1))^i \\
&+ (k_2 - 1)(P(X_1^{(1)} = 1))^{n_1+2} \\
&+ \sum_{i=n_1+3}^{n_1+n_3+2} (P(X_1^{(1)} = 1))^i \\
&+ (k_3 - 1)(P(X_1^{(1)} = 1))^{n_1+n_3+3}.
\end{aligned} \tag{2}$$

Here the first term represents the initially infected node and the second term represents the expected number of infected nodes in the star of the node 1, whereas the third term with the sum gives the expected number of the infected nodes in the rest of the chain between nodes 1 and 2, including the node 2. The fourth term depicts the number of infected nodes in the rest of the star of the node 2, the fifth term with the sum represents the number of infected nodes in the rest of the chain between the nodes 2 and 3, including the node 3, and the final sixth term gives the number of infected nodes in the rest of the star of the node 3.

The expected value of infected nodes in the second scenario is:

$$\begin{aligned}
E(Y_2) &= 1 + k_2 P(X_1^{(1)} = 1) + \sum_{i=2}^{n_1+1} (P(X_1^{(1)} = 1))^i \\
&+ (k_1 - 1)(P(X_1^{(1)} = 1))^{n_1+2} + \sum_{i=2}^{n_3+1} (P(X_1^{(1)} = 1))^i \\
&+ (k_3 - 1)(P(X_1^{(1)} = 1))^{n_3+2},
\end{aligned} \tag{3}$$

with respective terms as defined in (2). A prominent feature of both expressions (2) and (3) is that their dependence on p and q is captured by a single variable $P(X_1^{(1)} = 1)$. The difference of expectations of Y_1 and Y_2 as a function of $P(X_1^{(1)} = 1)$ is presented in Fig. 3.

For small values of $P(X_1^{(1)} = 1)$ the expectation of Y_1 dominates the expectation of Y_2 , but at larger values of $P(X_1^{(1)} = 1)$ the expected value of Y_2 is larger than the expected value of Y_1 . For $P(X_1^{(1)} = 1) = 0$ and $P(X_1^{(1)} = 1) = 1$ the expectations of these variables are equal.

Fig. 3 shows that for $P(X_1^{(1)} = 1) = 0$ there is no spreading of the disease. For small values of $P(X_1^{(1)} = 1)$ the spreading of the disease is contained and limited to the nearest neighbors. As $k_1 > k_2$, the expectation of $Y_1 - Y_2$ is positive. As $P(X_1^{(1)} = 1)$ grows, the disease progresses along the chains and for a sufficiently large $P(X_1^{(1)} = 1)$ the disease reaches the end of the chains. For a scenario with node 1 as the origin of the disease, in the regime of large $P(X_1^{(1)} = 1)$ the disease spreads to the node 2 and its star. However, the disease does not spread to the node 3 and its star. On the other hand, when the disease originates in node 2, owing to the central position of that node the disease spreads to both nodes 1 and 3 and their respective stars in the regime of sufficiently large $P(X_1^{(1)} = 1)$. That is why the expectation of $Y_1 - Y_2$ becomes negative in this regime. Finally, for $P(X_1^{(1)} = 1) = 1$ the disease spreads to the entire network in both scenarios and the expectations of Y_1 and Y_2 are equal to the total number of nodes in the network.

The analysis of the disease spreading in the network given in Fig. 2 serves as an illustration how the dependence of the node's epidemic ranking on the dynamical regime of spreading might be realized. It is reasonable to assume that this mechanism is just one of a broad class of mechanisms leading to dynamical

dependence of the epidemic ranking. Some of these mechanisms should also be effective in networks with cycles.

The dependence of the epidemic ranking of a node on the disease spreading dynamical regime has important implications in situations where some preparative action needs to be taken before the dynamical regime of disease spreading is known. An example of such a situation is the design of security and public health systems for countering the disease spreading. These protective system should, at least to some extent, function for virtually all disease spreading regimes. Some sort of average epidemic ranking, with averaging taken over all disease spreading regimes, becomes an essential ingredient for decisions on the structure of protective systems and efficient mitigation strategies. On the other hand, knowing some average impact of a node over all disease spreading regimes is important in its own right as a measure of epidemic importance of a node in the network. A useful framework for the calculation of the needed averages, the *phase diagram of epidemic spreading*, is described in the following subsection. The averaging procedures which take into account the dependence of the ranking on the dynamical regime of spreading are discussed in the final subsection of this section.

Phase diagram of epidemic spreading

For a fixed underlying complex network and a fixed initially infected node the outcome of the disease spreading still strongly depends on the properties of the disease itself, measured by parameters p and q in the SIR epidemic model. A very useful concept for the understanding and representation of the epidemic impact in the studied complex network for different values of p and q and a fixed initially infected node, named *the phase diagram of epidemic spreading*, has been recently introduced in [20].

In the phase diagram of epidemic spreading we consider the parametric space of the SIR model which is a $[0, 1] \times [0, 1]$ square. For each variable chosen to measure the impact of disease spreading a phase diagram can be constructed. Such variables useful in describing the impact of disease spreading are e.g. the average number of infected nodes (i.e. the final size of the epidemic) or the cumulative probability for a finite epidemic range [20]. The phase diagram of epidemic spreading is constructed in the following way: for each pair of allowed (p, q) parameters a value of the variable $X_{p,q}$ measuring the extent of disease spreading is determined (analytically or in simulations) and all triplets $(p, q, X_{p,q})$ are organized in a single diagram.

The phase diagram of epidemic spreading provides valuable insight into the bimodal character of disease spreading, i.e. equilibrium between the local containment of the disease and epidemic outbreak affecting the entire system [20]. Furthermore, it is a useful tool for searching for generic properties of disease spreading across different complex networks and initially infected nodes [20]. Finally, the phase diagram of epidemic spreading provides a global insight into a full set of disease spreading regimes. With a phase diagram of epidemic spreading available, one just needs to decide which averaging procedure is relevant and should be applied for the ranking calculation.

Epidemic centrality - an epidemic impact measure

To take into account the dependence of the epidemic ranking on the disease spreading dynamical regime, it is necessary to find a robust way to combine the effects of the entire parametric space, as stated in the preceding subsection. The concept of phase diagram of epidemic spreading lends itself as a natural framework for the definition of such a robust combination. Namely, a natural candidate for the measure of epidemic impact is some weighted average of the phase diagram of epidemic spreading over parametric space. We call this measure of epidemic impact *epidemic centrality* and for the node i we denote it by Z^i .

The simplest option is the uniform weight function. All disease spreading regimes are taken with equal weights in the calculation of the ranking (epidemic centrality), allowing us to express the epidemic

centrality Z^i as an integral over parametric space. In particular, for the SIR model one obtains

$$Z^i = \int_0^1 dp \int_0^1 dq X_{p,q}^i. \quad (4)$$

The assumption of uniform weighing of all disease spreading regimes could be contested as overly simplifying since a large majority of known contagious diseases have comparable or at least not drastically different transmission rates and average recovery times. Still, recent attempts of synthesis of artificial microorganisms [26] and nonspecific transmission patterns of some diseases among amphibian populations [27] warn us that diseases with nonstandard spreading regimes might pose significant risks in the future. These observations support uniform weighting of all spreading regimes in the averaging procedure of ranking calculation. In any case, (4) is a good starting point which should provide a good approximation of the ranking.

In general, the averaging should be performed using some nonuniform weight function $w(p, q)$. All available additional information on the epidemic risks posing a threat should be incorporated into that function. For example, if it is known that the spreading regimes of the diseases posing the greatest threat are constrained to a segment of the parametric space, then the weight function should have a peak in this part of the parametric space. The epidemic centrality is then calculated as

$$Z^i = \int_0^1 dp \int_0^1 dq w(p, q) X_{p,q}^i. \quad (5)$$

The procedure of calculation of epidemic centrality is schematically depicted in Fig. 4. The idea of proper averaging over different disease spreading parameters has been recently also addressed in SIS model [9]. In that paper, Youssef et al. argue that measures such as the epidemic threshold or the number of infected nodes in the asymptotic steady state, taken separately, do not give the appropriate measure of network robustness to epidemic. They introduce a useful novel measure, defined at the level of the entire network, which they call *viral conductance* (VC). Viral conductance is essentially an average of number of infected nodes in the asymptotic steady state for all SIS model parameters above epidemic threshold. The similarity of the concepts of viral conductance for SIS model and epidemic centrality for SIR model lies in the premise that numbers of infected nodes for various disease spreading parameters need to be combined to obtain relevant measures of importance of network topologies (in the case of viral conductance) or node positions (in the case of epidemic centrality) in disease spreading. However, viral conductance and epidemic centrality are defined for SIS and SIR, respectively, which are substantially different models used for modeling of spreading of different diseases. The concept of epidemic centrality is defined for *every* individual node in the network and it furthermore allows the ranking of the nodes according to their epidemic impact. The concept of viral conductance, on the other hand, is defined at the level of the entire network structure. Finally, the motivation for the introduction of epidemic centrality is a much broader phenomenon of dependence of epidemic ranking on disease spreading parameters, discussed in detail in this paper. The concept of viral conductance is largely complementary to epidemic centrality, given their different properties and areas of applicability. Nevertheless, the proposal of Youssef et al. in SIS, along with the concept of epidemic centrality introduced in our paper, reasserts the need to evaluate the importance of network structure in disease spreading for many disease spreading parameters simultaneously.

Results and Discussion

We first focus on results obtained using the uniform weight function (4). Although our main discussion is focused on the comparison of epidemic centrality with structural measures such as node degree, we would like to stress that epidemic centrality is a well defined and motivated measure of the epidemic

impact on its own. The said comparison does not serve as a validation of the epidemic centrality, but as a part of analysis on the importance of the nodes which are structurally peripheral and the nodes which are structurally central. The dependence of epidemic centrality on the node degree is studied for four empirical complex networks (astro-ph, cond-mat 2003, internet, power grid) and their respective epidemic centralities are shown in Fig. 5. All studied networks share some common properties. The epidemic centrality in general grows with the degree of the initially infected node although considerable scattering for the same degree exists. The average of epidemic centralities of all nodes with the same degree grows with the degree of the initially infected node, whereas the standard deviation as a measure of scattering decreases with the degree of the initially infected node, as depicted in Fig. 5. For astro-ph, cond-mat 2003 and internet networks the scattering reduces considerably for high degree nodes and for power-grid network scattering is present even for the high degrees.

The dependence of epidemic centrality of infected nodes on the k-cores variable of each initially infected node for the four studied networks is presented in Fig. 6. For astro-ph, cond-mat 2003 and internet networks, the epidemic centrality in general grows with k-cores of initially infected nodes. As depicted in Fig. 6, the epidemic centrality of initially infected nodes with the same k-cores value grows with the k-cores, whereas the standard deviation as a measure of scattering decreases with the k-cores value. The power grid network exhibits somewhat different behavior. Namely, the epidemic centrality of initially infected nodes with the same k-cores value first increases and then decreases, but the standard deviation decreases with the k-cores values. The interpretation of this peculiarity is obscured by a very small range of k-cores values present in the power grid network.

The dependence of epidemic centrality on betweenness of the initially infected nodes for four studied networks is displayed in Fig. 7. From all these four figures it is evident that there is no clear relation between the epidemic centrality and betweenness of the initially infected node. Although no clear relation between the epidemic centrality and the betweenness of the initially infected nodes can be identified, it is striking that the patterns in all plots in Fig. 7 are very similar in general and exhibit very similar peculiar details. In particular, in all studied networks there are two intervals of betweenness where epidemic centrality has dispersion larger than average: the first at small values of betweenness and the second close to the largest values of betweenness for the studied network.

Finally, the dependence of epidemic centrality on degree and k-cores value of the initially infected node for the simulated Erdos-Renyi networks is presented in Fig. 8. This figure clearly shows a qualitatively same dependence of epidemic centrality on the studied structural variables. This finding indicates that the observed properties of epidemic centrality are not restricted to the studied empirical complex networks or networks with broad degree distributions. Establishing a possible universality of some epidemic centrality properties over broad classes of networks would, however, require a far more extensive study which is beyond the scope of this paper.

Although the relation between epidemic centrality on the one hand and structural variables such as degree and k-cores on the other hand is clearly nonlinear, it is also important to know how similar are rankings based on degree or k-cores value to the epidemic ranking based on epidemic centrality. To establish this similarity we relabel nodes according epidemic ranking (the highest ranked node is relabeled 1 and the i^{th} ranked node is relabeled as i) and then produce the sequence of rankings according to degree (or k-cores value) and to each node i we assign the structural ranking $r_{\text{struct}}(i)$. Then we calculate Spearman's rank correlation coefficient of sequences i and $r_{\text{struct}}(i)$. The results for the studied networks are presented in Table 1. The obtained results show that for astro-ph, cond-mat 2003 and internet networks ranking based on degree or k-cores value is very similar to epidemic ranking. For the power grid network the correlation is notably lower, but still considerable.

The most interesting feature observed in all networks discussed in this section is a very small ratio of the largest and the smallest epidemic centrality in the network. The epidemic centrality of nodes that are completely peripheral in the structure of the network (either in terms of their degree or k-cores value) is only about a factor 2 smaller than the epidemic centrality of the nodes that we would describe as central

from the structural point of view. Given that the variation in degree in all studied networks (except power grid) goes up to several orders of magnitude and that k-cores variable acquires values of more than 20, it is intriguing that the epidemic centrality is so insensitive to this variation.

A reasonable question is how much the findings of the preceding paragraph depend on the choice of the weight function. In particular, it would be important to learn if the relative insensitivity of epidemic centrality on structural variables is a consequence of the uniform weight function, see (4). As there is an unlimited number of choices for the nonuniform weight function, we restrict ourselves to beta distribution $f_{\alpha,\beta}(x) = \frac{\Gamma(\alpha+\beta)}{\Gamma(\alpha)\Gamma(\beta)}x^{\alpha-1}(1-x)^{\beta-1}$ [28] as a sufficiently broad class able to approximate well any weight function that might be of interest.

We find that the qualitative conclusions presented for the uniform $w(p, q)$ hold also for other weight functions localized in specific parts of the parametric space. To demonstrate this, we choose four weight functions $w(p, q)$ which are well localized in four quadrants of the (p, q) parametric space. We select the weight functions of the form $w(p, q; \alpha_1, \beta_1, \alpha_2, \beta_2) = f_{\alpha_1, \beta_1}(p) \cdot f_{\alpha_2, \beta_2}(q)$, where $f_{\alpha, \beta}(x)$ is the beta distribution. Particular forms of the functions are $w_A(p, q) = w(p, q; \alpha_1 = 30, \beta_1 = 10, \alpha_2 = 10, \beta_2 = 30)$, $w_B(p, q) = w(p, q; \alpha_1 = 30, \beta_1 = 10, \alpha_2 = 30, \beta_2 = 10)$, $w_C(p, q) = w(p, q; \alpha_1 = 10, \beta_1 = 30, \alpha_2 = 10, \beta_2 = 30)$, and $w_D(p, q) = w(p, q; \alpha_1 = 10, \beta_1 = 30, \alpha_2 = 30, \beta_2 = 10)$, which are presented in Fig. 9. For the cond-mat 2003 network, the relation of the node degree and the average epidemic centrality for that node degree is given in Fig. 10 for the four choices for the weight function. Although the range of values of average epidemic centrality varies with the chosen weight function, the average epidemic centralities remain of the same order of magnitude even as the degree varies several orders of magnitude. An equivalent conclusion can be drawn on the relation of the k-cores value and the average epidemic centrality for a particular k-cores value. Furthermore, equivalent conclusions can be reached for astro-ph, internet and power networks. It is important to observe that for the small values of p and large values of q (in particular for the weight function $w_D(p, q)$) the values of epidemic centrality for some nodes of small degree may become rather small (much smaller than the average epidemic centrality for a given degree). However, the average epidemic centrality (and a majority of epidemic centrality values of individual nodes) remains of the same order of magnitude as for the large degrees.

To further elaborate on the dependence of our results on the choice of weight function and the problem of similarity/distinction of uniform and nonuniform weight functions, we consider the following analysis. We consider a family of weight functions $w(p, q) = f_{\alpha, \alpha}(p)f_{\alpha, \alpha}(q)$ that contains a uniform weight function as a special case for $\alpha = 1$ and $f_{\alpha, \alpha}(x)$ is symmetrically centered around its expectation value $x = 1/2$. Starting from $\alpha = 1$ and increasing the value of α we go from the uniform weight functions to the more and more localized ones. The value of α serves as a measure of localization of the weight function. For each of α values we calculate the ratio of maximal and minimal average epidemic centrality for nodes with the same degree and plot this ratio as a function of α . These plots for all studied networks are presented in Fig. 11. For astro-ph, cond-mat 2003 and internet networks even for very localized weight functions the studied ratio remains very close to its value for the uniform weight function. In the case of power grid network, the ratio grows with localization, although at a decreasing rate. As already observed at other places in this paper, the power grid exhibits different behavior than other studied complex networks. A possible interpretation of this difference might lie in the fact that the degree distribution for the power grid network is exponential, whereas other empirical complex networks have a broad degree distribution.

The studies presented so far point to a somewhat surprising general conclusion with very important practical consequences. The epidemic centrality as an average measure of epidemic impact is much more homogeneous among nodes of studied networks than are its structural properties. In the studied networks, the epidemic centrality of a node does show growing trends with its degree and k-cores value, but with a rather low sensitivity to these structural variables. For example, whereas the degree of nodes may differ several orders of magnitude, the epidemic centrality changes within the factor of a few. A natural conclusion imposing itself is that, as far as the epidemic centrality could be taken as a measure of the epidemic impact, the importance of structurally peripheral nodes in the studied networks should be much

higher than their structural variables might imply. Although our conclusions on the importance of the structurally peripheral nodes can be strictly applied only to networks and weight functions studied in this paper, a diverse character of studied complex networks (empirical vs. synthetic, ER vs. networks with broad degree distributions) and weight functions (uniform vs. localized), indicates that underestimated epidemic impact of structurally peripheral nodes might be a phenomenon valid in epidemic spreading in the SIR model in a much broader class of complex networks.

The problem of allocation of resources dedicated to countering the disease spreading (see e.g. [29,30]) should be definitely strongly influenced by our findings on epidemic centrality. If we adopt a strategy that the amount of resources allocated to a certain node should be proportional to its epidemic centrality, then a logical conclusion is that virtually all nodes in the network should receive comparable amount of resources. Another implication is that allocating a lot of resources to hubs and nodes with high k-cores values does not necessarily make the entire network more resilient to epidemic outbreaks. To the contrary, the allocation of large amounts of resources to structurally central nodes necessarily leaves structurally peripheral nodes without resources although they are associated to a comparable epidemic impact.

The findings of the preceding paragraph rest on a simple assumption that the disease spreading can be contained only at its source. i.e. the initially infected node. In that case it is necessary to allocate as much resources to the node as the epidemic impact would be if the disease escaped the initially infected node. This assumption is certainly only approximately true, but in our opinion it captures the leading contribution to the risk associated with the epidemic. Moreover, it is especially applicable to the class of situations of a newly introduced and rapidly spreading pathogen when standard resources such as vaccines and medicines are not available.

The finding that the nodes having very different structural variables actually have comparable epidemic centralities does not imply that the roles of these nodes in the process of disease spreading are the same. The fact that two nodes N and M have comparable epidemic centralities just means that the mean number of infected nodes, appropriately averaged over the parametric space, will be comparable if the disease spreading starts at the node M or the node N . In the actual process of spreading, hubs have a far more prominent role than the peripheral nodes. If the disease spreading starts at a peripheral node, the spreading is slow until the disease reaches some of the hubs and then the spreading (measured by the number of infected nodes) accelerates. The epidemic centrality describes the final outcome of the epidemic and not its precise temporal development.

Finally, entire discussion in this section was focused on the implications of the introduced concept of epidemic centrality in epidemiology. Our findings also apply to e.g. problems of spreading of ideas and trends in social networks. The relative insensitivity of epidemic centrality (or its counterpart in spreading of ideas and trends in social networks) to structural measures of centrality such as node degree or k-cores value might play an important role in understanding of social dynamics on these networks. The possibility that the capacity of spreading of new ideas or imposing new trends might not be an exclusive privilege of highly connected nodes deserves further elaboration.

In conclusion, the structure of spreading pathways and the dynamics of disease transmission are intertwined in a very complex way. Any ranking of nodes according to epidemic impact based exclusively on structural arguments is therefore inadequate. The first principal result of this paper is that the epidemic ranking depends crucially on the disease spreading regime. If we are interested in finding some ranking of initially infected nodes that does not depend on specific spreading regime, the entire parametric space has to be taken into account using appropriate averaging procedures. We introduce epidemic centrality as a measure of epidemic centrality based on averaging over entire parametric space. The second major result of this paper is that the variation of epidemic centrality of initially infected nodes is much smaller than the variation of their degrees or k-cores values. This finding indicates that the epidemic risk associated to the structurally peripheral nodes might be much larger than their degrees or k-cores values would imply. If the spreading of the disease can be stopped only at its source, the optimal distribution of resources dedicated to stopping the spreading should be proportional to epidemic

centralities of the initially infected nodes. The concept of epidemic centrality merits further elaboration and its extension to other epidemiological models and more realistic complex networks. These tasks, together with the application of these results beyond epidemiology represent short term goals of future research.

Acknowledgments

The authors would like to thank Petra Klepac for valuable comments on the manuscript and useful pointers to the literature. The work of M. Š. is financed by Biomedical Research Council of A*STAR, Singapore and by Ministry of Education Science and Sports of the Republic of Croatia under Contract No. 036-0362214-1987 and 098-1191344-2860. The work of H. Š. is supported by the Ministry of Education Science and Sports of the Republic of Croatia under Contract No. 098-0352828-2863.

References

1. Anderson RM, May RM (1991) *Infectious Diseases of Humans: Dynamics and Control*. Oxford University Press.
2. Keeling MJ, Rohani P (2008) *Modeling Infectious Diseases in Humans and Animals*. Princeton University Press.
3. Pastor-Satorras R, Vespignani A (2001) *Phys Rev Lett* 86: 3200.
4. Albert R, Barabási AL (2002) *Rev Mod Phys* 74: 47.
5. Newman MEJ (2003) *SIAM Rev* 45: 167.
6. Dorogovtsev SN, Goltsev AV, Mendes JFF (2008) *Rev Mod Phys* 80: 1275.
7. Grassly NC, Fraser C (2008) *Nature Reviews (Microbiology)* 6: 477.
8. Boccaletti S, Latora V, Moreno Y, Chavez M, Hwang DU (2006) *Phys Rept* 424: 175.
9. Youssef M, Kooij R, Scoglio C (2011) *Journal of Computational Science* 2: 286.
10. Colizza V, Barrat A, Barthelemy M, Valleron AJ, Vespignani A (2007) *Plos Medicine* 4: 95.
11. Colizza V, Barrat A, Barthelemy M, Vespignani A (2006) *Proc Natl Acad Sci USA* 103: 2015.
12. Colizza V, Vespignani A (2007) *Phys Rev Lett* 99: 148701.
13. Kitsak M, Gallos LK, Havlin S, Liljeros F, Muchnik L, et al. (2010) *Nature Phys* 6: 888.
14. Freeman LC (1979) *Social Networks* 1: 215.
15. Friedkin NE (1991) *Am J of Sociology* 96: 1478.
16. Shen Z, et al (2004) *Emerg Infect Dis* 10: 256.
17. Lloyd-Smith JO, Schreiber SJ, Kopp P, Getz WM (2005) *Nature* 438: 355.
18. Bansal S, Grenfell BT, Meyers LA (2007) *J R Soc Interface* 4: 879.
19. Kermack WO, McKendrick AG (1927) *Proc Roy Soc Lond A* 115: 700.

20. Lancic A, Antulov-Fantulin N, Sikic M, Stefancic H (2011) *Physica A* 390: 65.
21. Volz E, Meyers LA (2009) *J R Soc Interface* 6: 233.
22. Schwartz IB, Shaw LB (2010) *Physics* 3: 17.
23. Newman MEJ (2001) *Proc Natl Acad Sci USA* 98: 404.
24. Watts DJ, Strogatz SH (1998) *Nature* 393: 440.
25. Newman MEJ. <http://www-personal.umich.edu/~mejn/netdata/>.
26. Gibson DG, et al (2010) *Science* 329: 52.
27. Vredenburg VT, Knapp RA, Tunstall TS, Briggs CJ (2010) *Proc Natl Acad Sci USA* 107: 9689.
28. http://en.wikipedia.org/wiki/Beta_distribution.
29. Forster GA, Gilligan CA (2007) *Proc Natl Acad Sci USA* 104: 4984.
30. Rowthorn RE, Laxminarayan R, Gilligan CA (2009) *J R Soc Interface* 6: 1135.

Figures

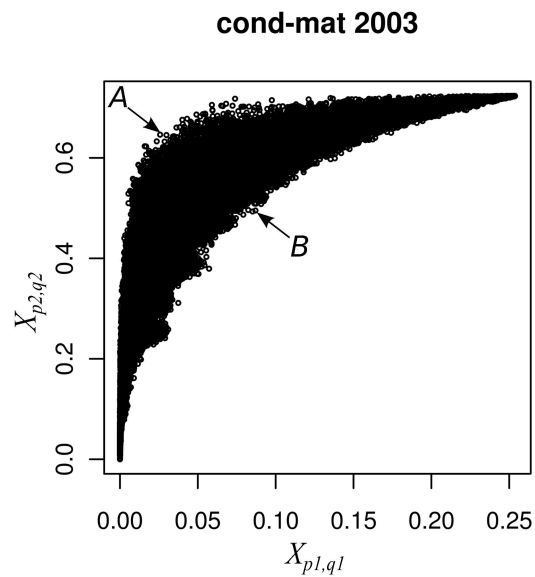


Figure 1. The mean number of infected nodes normalized to the total number of nodes in the network in the regime $(p_1 = 0.1, q_1 = 0.9)$ (on the x-axis) versus the mean number of infected nodes normalized to the total number of nodes in the network in the regime $(p_2 = 0.1, q_2 = 0.2)$ (on the y-axis) for the cond-mat complex network and the same initially infected node. For a very large number of node pairs their relative epidemic ranking changes when the first regime is changed to the second one. Points *A* and *B* marked in the plot give a clear example of such a pair.

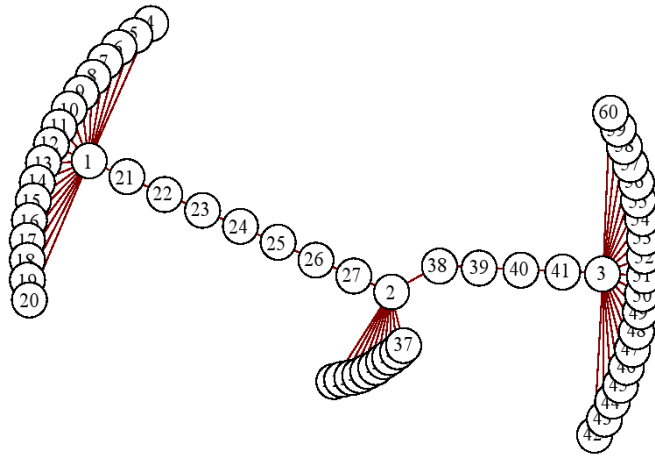


Figure 2. The artificial network with three distinguished nodes 1, 2, and 3 with parameters $k_1 = 18$, $k_2 = 12$, $k_3 = 20$, $n_1 = 7$ and $n_3 = 4$ as defined in the text (Online version in colour).

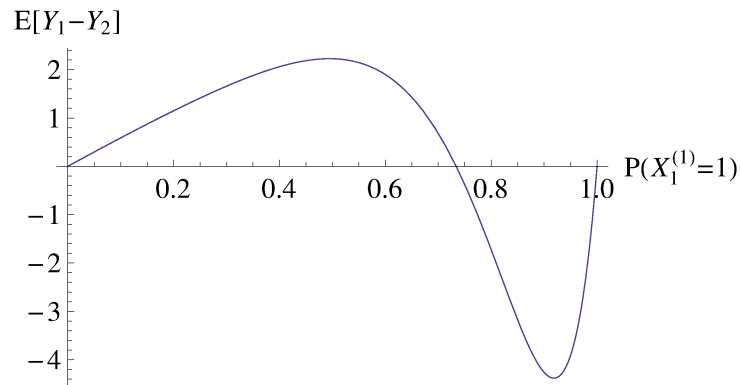


Figure 3. The difference of the expected numbers of infected nodes for scenarios where the node 1 is the initially infected node (Y_1) and the node 2 is the initially infected node (Y_2) (Online version in colour).

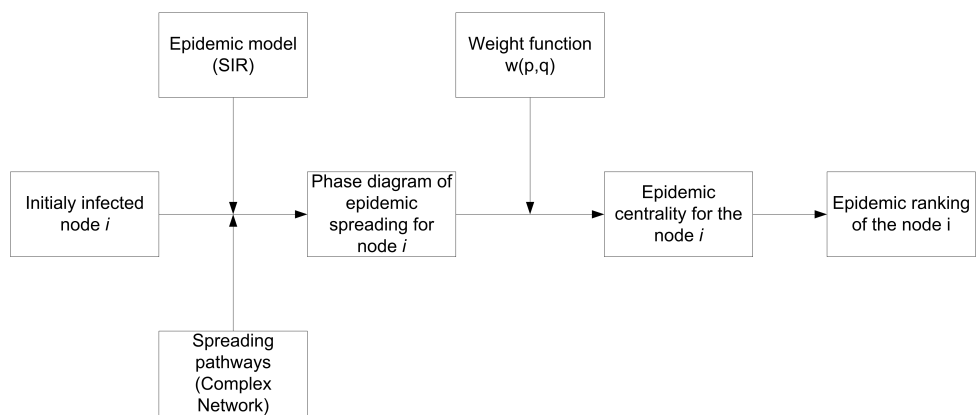


Figure 4. The schematic representation of the procedure for the calculation of epidemic centrality.

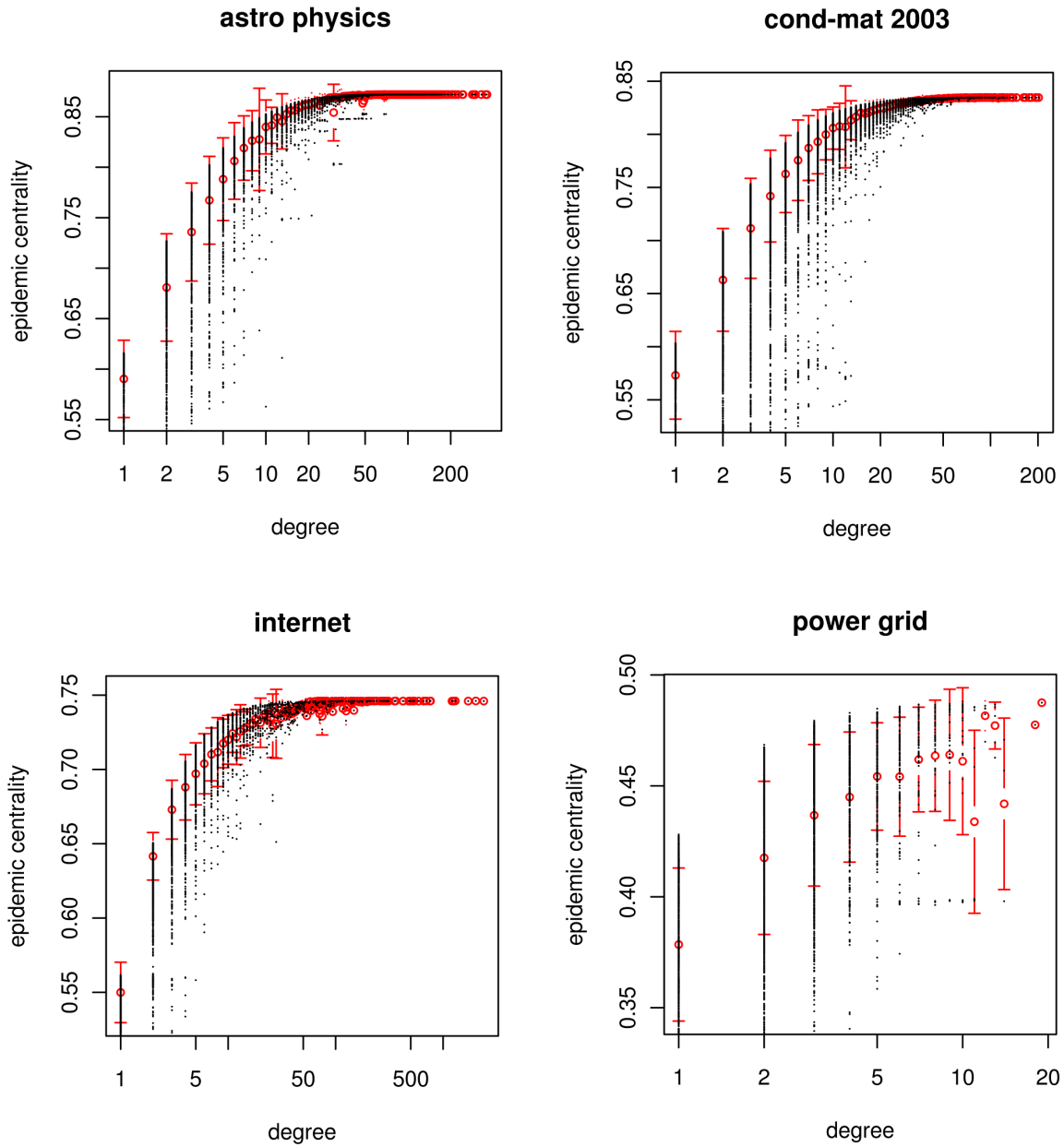


Figure 5. The epidemic centrality versus the degree of the initially infected node for the studied empirical complex networks: astro-ph (top left), cond-mat 2003 (top right), internet (bottom left) and power grid network (bottom right). Black dots represent epidemic centrality values of individual nodes and red circles with error bars represent the average value and the standard deviation of epidemic centrality for a given degree.

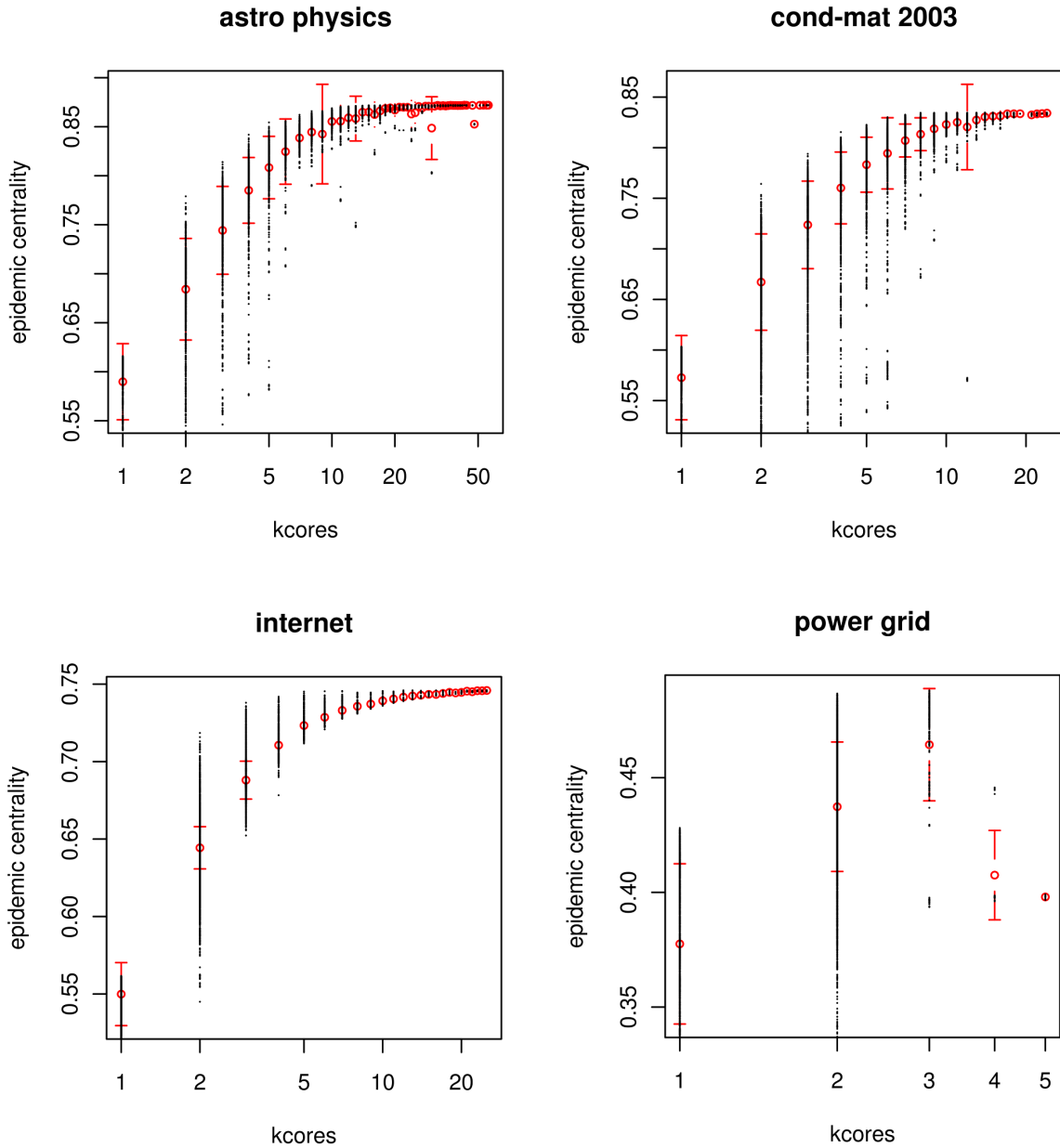


Figure 6. The epidemic centrality versus the k-cores of the initially infected node for the studied empirical complex networks: astro-ph (top left), cond-mat 2003 (top right), internet (bottom left) and power grid network (bottom right). Black dots represent epidemic centrality values of individual nodes and red circles with error bars represent the average value and the standard deviation of epidemic centrality for a given k-cores value.

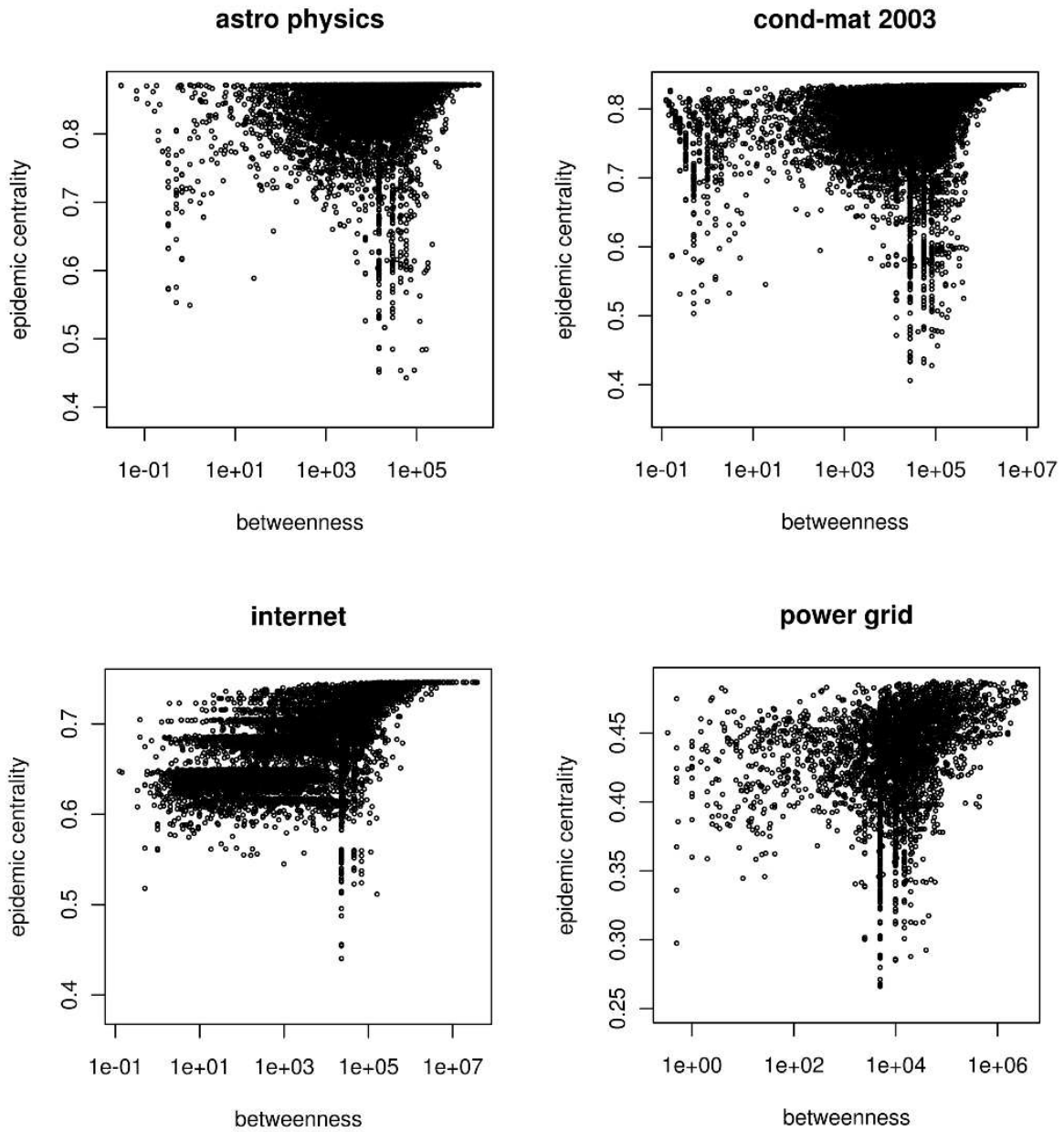


Figure 7. The epidemic centrality versus the betweenness of the initially infected node for the studied empirical complex networks: astro-ph (top left), cond-mat 2003 (top right), internet (bottom left) and power grid network (bottom right).

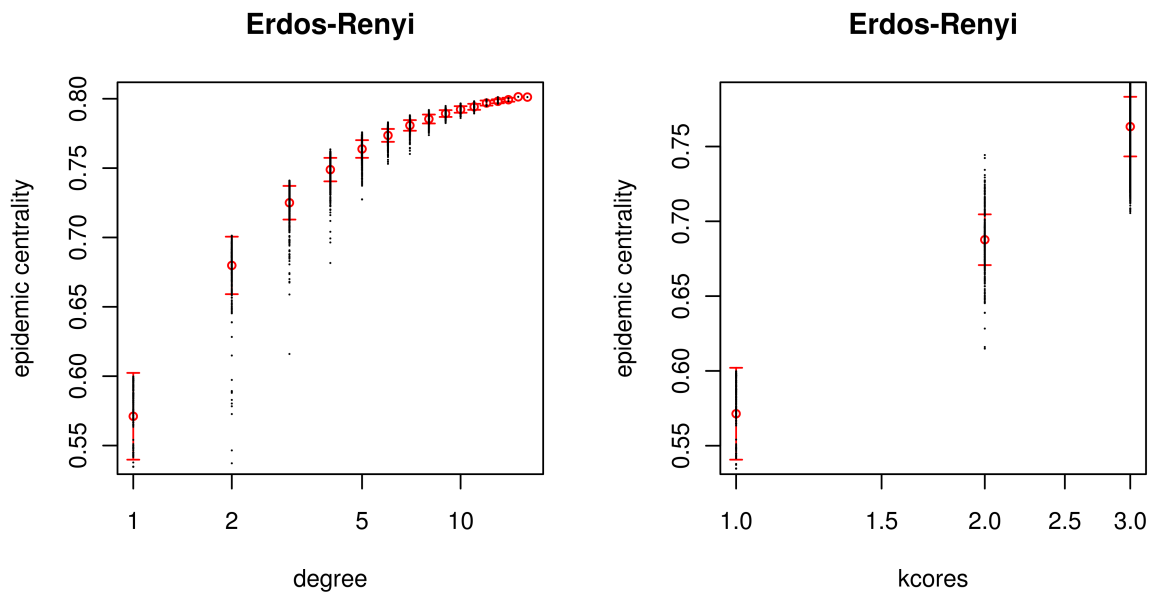


Figure 8. The epidemic centrality versus the degree (left) and the k-cores (right) of the initially infected node for an Erdos-Renyi network $G(5000, 0.001)$.

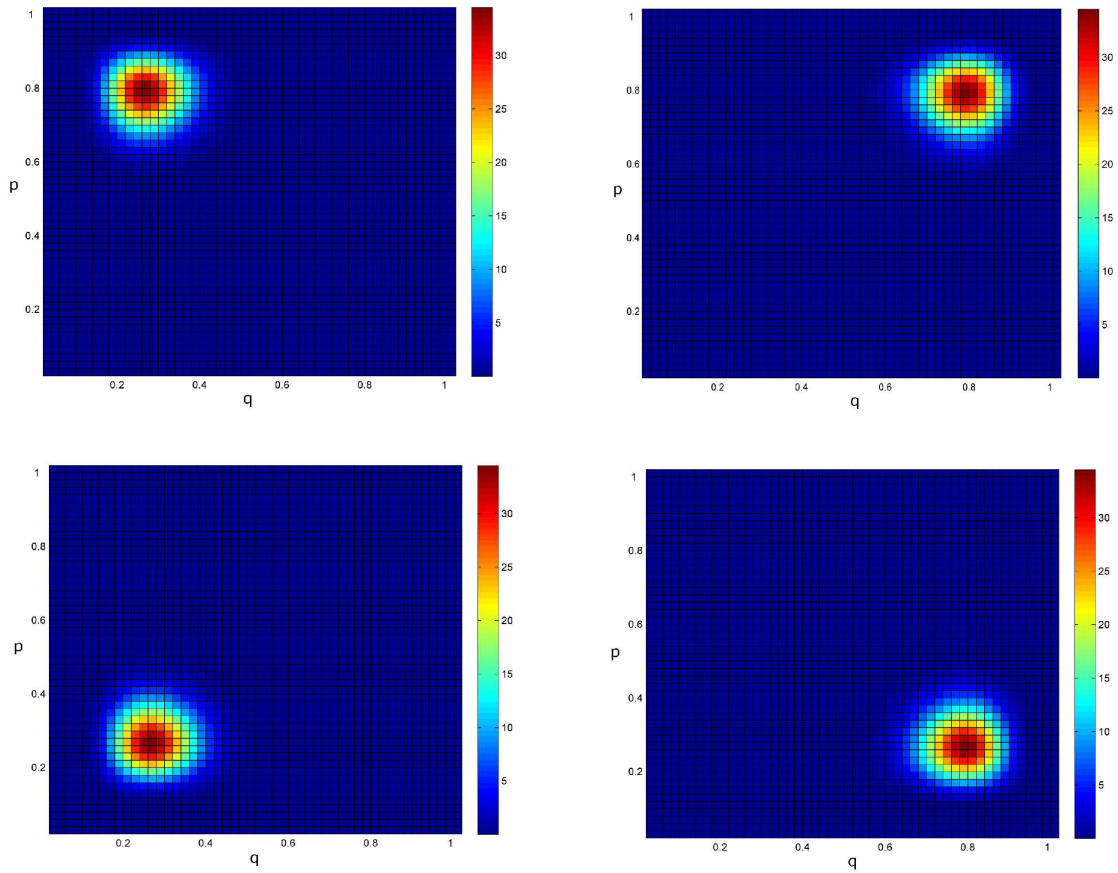


Figure 9. Contour plots of four weight functions localized in the region of small q and large p ($w_A(p, q)$, top left), large q and large p ($w_B(p, q)$, top right), small q and small p ($w_C(p, q)$, bottom left) and large q and small p ($w_D(p, q)$, bottom right). For the definitions of $w_{A,B,C,D}(p, q)$ see the section Results and Discussion.

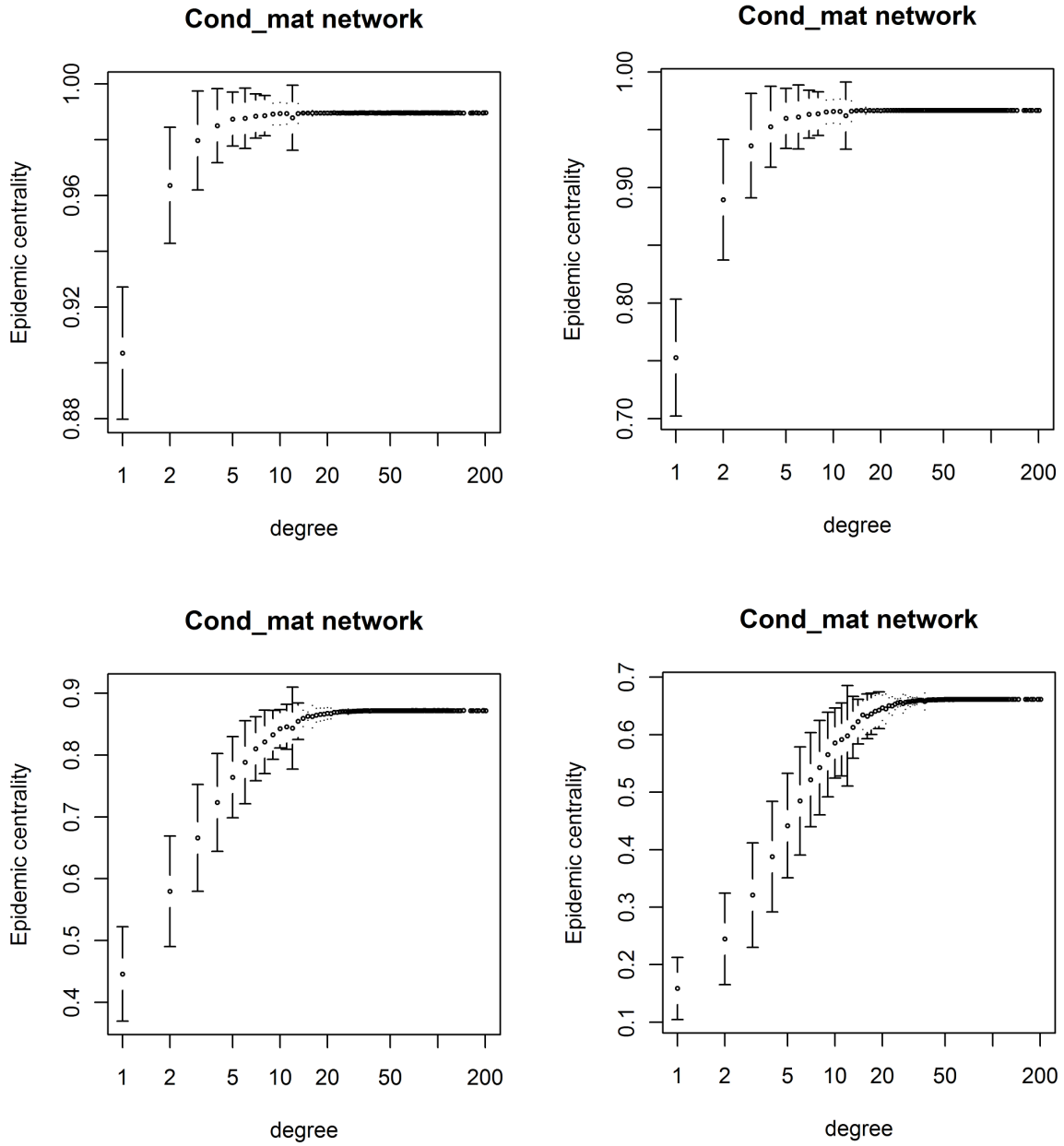


Figure 10. The average values and standard deviations of epidemic centrality versus node degree for cond-mat 2003 network for four different weight functions depicted in Fig. 9.

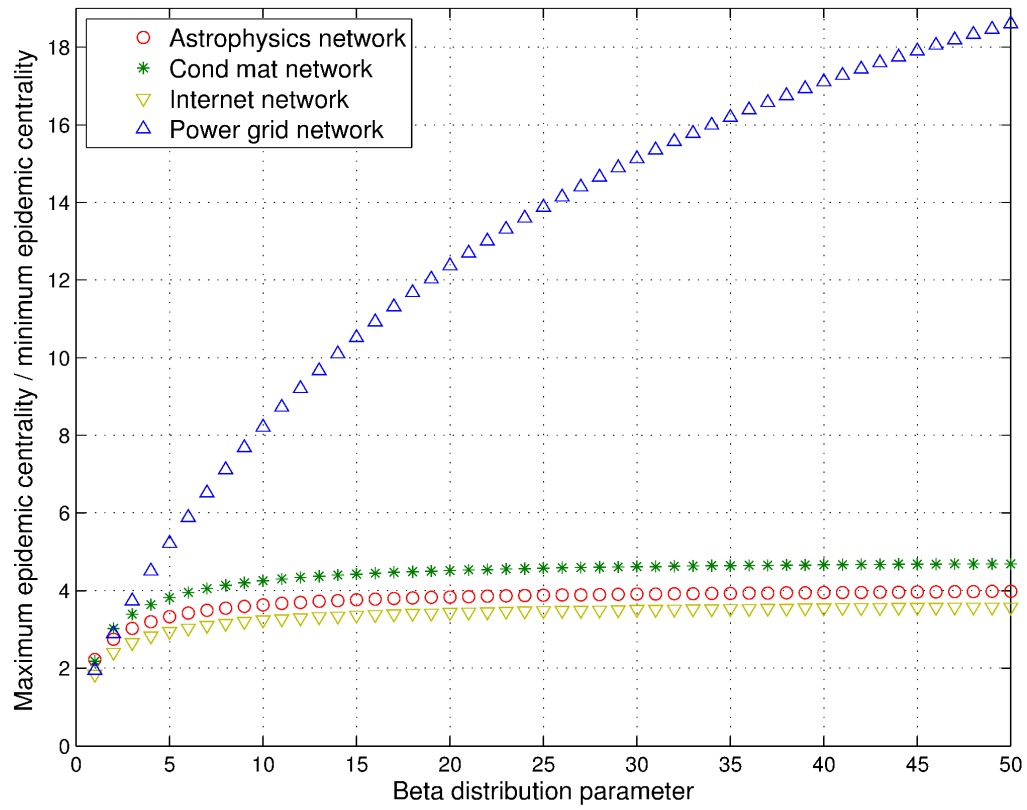


Figure 11. The ratio of maximal to minimal average epidemic centrality of nodes with the same degree for four studied networks for different localizations of the weight function measured by the parameter α (Online version in colour).

Tables

Table 1. Spearman's rank correlation coefficient of epidemic ranking and ranking based on node degree or k-cores value for four studied complex networks.

	degree	k-cores
astro-ph	0.97	0.96
cond-mat	0.94	0.93
internet	0.91	0.92
power grid	0.66	0.68